Modulation of the canonical Wnt signaling pathway in bone and cartilage

Miclea, R.L.

Chapter 4

Apc bridges Wnt/β-catenin and BMP signaling during osteoblast differentiation of KS483 cells

R.L. Miclea[1], G. van der Horst[2], E.C. Robanus-Maandag[3], C.W. Löwik[4], W. Oostdijk[1], J.M. Wit[1], M. Karperien[5]

[1]Department of Pediatrics, Leiden University Medical Centre (LUMC), Leiden, The Netherlands, [2]Department of Urology, LUMC, Leiden, The Netherlands, [3]Department of Human Genetics, LUMC, Leiden, The Netherlands, [4]Department of Endocrinology and Metabolic Diseases, LUMC, Leiden, The Netherlands, [5]MIRA Institute for Biomedical Technology and Technical Medicine, Department of Tissue Regeneration, University of Twente, Enschede, The Netherlands

Exp Cell Res. 2011 Jun 10;317(10):1411-21

Apc bridges Wnt/β-catenin and BMP signaling during osteoblast differentiation of KS483 cells

R.L. Miclea, G. van der Horst, E.C. Robanus-Maandag, C.W. Löwik, W. Oostdijk, J.M. Wit, M. Karperien

ABSTRACT

The canonical Wnt signaling pathway influences the differentiation of mesenchymal cell lineages in a quantitative and qualitative fashion depending on the dose of β-catenin signaling. Adenomatous polyposis coli (Apc) is the critical intracellular regulator of β-catenin turnover.

To better understand the molecular mechanisms underlying the role of Apc in regulating the differentiation capacity of skeletal progenitor cells, we have knocked down *Apc* in the murine mesenchymal stem cell-like KS483 cells by stable expression of *Apc*-specific small interfering RNA. In routine culture, KSFrt-Apc_{si} cells displayed a mesenchymal-like spindle shape morphology, exhibited markedly decreased proliferation and increased apoptosis. *Apc* knockdown resulted in upregulation of the Wnt/β-catenin and the BMP/Smad signaling pathways, but osteogenic differentiation was completely inhibited. This effect could be rescued by adding high concentrations of BMP-7 to the differentiation medium. Furthermore, KSFrt-Apc_{si} cells showed no potential to differentiate into chondrocytes or adipocytes.

These results demonstrate that Apc is essential for the proliferation, survival and differentiation of KS483 cells. *Apc* knockdown blocks the osteogenic differentiation of skeletal progenitor cells, a process that can be overruled by high BMP signaling.

INTRODUCTION

During endochondral bone formation, skeletal progenitor cells (SPC) arise from mesenchymal cells, transit several differentiation steps to ultimately develop into bone or cartilage (1). Their commitment to one of the two lineages requires a very intricate and tightly controlled crosstalk between transcription factors, cytokines, and growth factors (2). However, the precise molecular interactions that control their lineage commitment and differentiation to mature skeletal cells are not fully understood.

Increasing evidence suggests an important role of the canonical Wnt signaling pathway in the regulation of lineage commitment of SPC (3). In this pathway, in the absence of the Wnt signal, cytoplasmic β-catenin is degraded in the proteasome upon its phosphorylation at specific Ser-Thr residues by a destruction complex consisting of Axin, Adenomatous Polyposis Coli (APC), Glycogen synthase kinase 3β (GSK3β) and Casein-kinase 1α (CK1α). Wnt growth factors bind to the receptor Frizzled and low-density lipoprotein receptor-related protein-5 or 6 (LRP-5/6) to inactivate this destruction complex, via Dishevelled (DVL). This leads to accumulation of unphosphorylated β-catenin and subsequent translocation into the nucleus. Together with members of the T cell factor/lymphoid enhancer factor (TCF/LEF) family, nuclear β-catenin stimulates transcription of Wnt target genes (4). Up-regulation of β-catenin in bi-potential SPC leads to osteoblast formation, whereas down-regulation favors their commitment to the chondrogenic lineage (5).

Another signaling cascade equally important in the differentiation of SPC is the bone morphogenetic protein (BMP)/Smad pathway which promotes both osteo- and chondrogenesis (6). In this pathway, BMPs bind to and activate BMP type I or II receptors thereby initiating phosphorylation of receptor-regulated Smads (R-Smads) 1, 5, and 8. Phosphorylated active R-Smads form heteromeric complexes with common-partner Smad4 that translocate to the nucleus to regulate the transcription of target genes in cooperation with other transcription factors (7).

Due to the great importance of the Wnt/β-catenin and BMP pathway during both osteogenic and chondrogenic differentiation of SPC, the interaction between these two powerful regulatory pathways has received much attention. For example, it has been shown that BMP-2 upregulates expression of Wnt-3a and β-catenin and that β-catenin is crucial for BMP-induced new bone formation (8;9). However, the BMP signal can also antagonize Wnt in SPC by promoting an interaction between Smad1 and Dvl that restricts β-catenin accumulation (10). These and other data suggest that Wnt and BMP signaling can alternatively synergize or antagonize one another in differentiation of SPC (11;12).

We have recently shown that, by downregulating the canonical Wnt/β-catenin signal, Apc is essential for the commitment of SPC to the chondrogenic and osteogenic lineage (13). Moreover, distinct *Apc* mutations unevenly affect the differentiation potential of mouse embryonic stem cells (ES): whereas *Apc* alleles entirely deficient in β-catenin downregulation domains block the differentiation potential of ES, more

hypomorphic alleles which are still able to partially downregulate β-catenin impair the differentiation of ES only to some tissues, e.g. bone and cartilage (14). In cells carrying a hypomorphic Apc mutation, the levels of β-catenin are upregulated only when Apc activity levels are below 2% of normal (14).

To further unravel the subtle role of Apc in the regulation of SPC differentiation, we have knocked down the mouse *Apc* gene using RNA interference (RNAi) in the murine mesenchymal stem cell-like KS483 cell line. This cell line shows SPC-like characteristics, since it can form osteoblasts, chondrocytes, and adipocytes (15). Our data suggest that *Apc* knockdown in KS483 cells leads to up-regulation not only of the Wnt/β-catenin, but also of the BMP signaling pathway, further sustaining the interaction of these biological routes during various steps of SPC differentiation. Low levels of Apc inhibited osteoblast, chondrocyte and adipocyte differentiation. Interestingly, the inhibitory effects of Apc knockdown on osteogenic differentiation could be rescued by high levels of BMP-7.

MATERIALS AND METHODS

Generation of the KS483 cell lines with stable expression of Apc_{si} constructs

To obtain the KSFrt-*Apc*$_{si}$ stable cell line, the *shRNA* plasmid p5H1-*Apc*$_{si}$, designed to express shRNA targeting the mouse *Apc* gene, was constructed as described previously (15). To obtain the control, KSFrt-mt*Apc*$_{si}$ stable cell line, the *shRNA* plasmid p5H1-mt*Apc*$_{si}$ was generated by introducing mismatches at position 7 and 15 of the *Apc* target sequence. To demonstrate the biological reproducibility of our results, the KSFrt-*Apc**$_{si}$ and the KSFrt-mt*Apc**$_{si}$ cell lines were also generated using the p5H1-*Apc**$_{si}$ and the p5H1-mt*Apc**$_{si}$ plasmid (carrying mismatches at position 5 and 16 of the *Apc**$_{si}$ construct), respectively. The target sequences used to specifically silence *Apc* (*Apc*$_{si}$, *Apc**$_{si}$) and their corresponding mutant (control) sequences (mt*Apc*$_{si}$, mt*Apc**$_{si}$) are shown in Figure 1A. Stable transfections of the 4C3 Frt clone of the KS483 murine host cell line were performed as previously described (15). In this clone, a unique Flp recombinase target (FRT) sequence is introduced in the genome. This site is subsequently used for targeted insertion of the short hair pin vector using Flp-mediated homologous recombination (15).

Cell culture

KS483 cells were routinely cultured in T75 culture flasks (Greiner Bio-One) as described previously (16). For the KSFrt 4C3 host cell line the medium was supplemented with blasticidin S HCl (2 μg/ml; Invitrogen). All stably transfected cell lines were cultured in the presence of hygromycin B (100 μg/ml; Invitrogen).

Immunofluorescence

Immunofluorescence for Apc and β-catenin was performed as described previously with minor modifications (16). In brief, cells were seeded on glass slides (BD Falcon) and either left untreated or treated with Wnt3a (30ng/ml; R&D Systems) for

3hrs. The primary antibodies were rabbit polyclonal anti-Apc (1:500 in NETGEL; Abcam) and rabbit polyclonal anti-β-catenin (1:500 in NETGEL; Abcam). The second antibody used was goat anti-rabbit FITC-conjugate (1:250; Sigma). The F-actin cytoskeleton was counterstained using Phalloidin-TRITC (0.33 mg/ml; Sigma). Cells were imaged using the 63× objective of an inverted Leica SP2 confocal microscope.

Western Blot

Approximately 2 x 10^7 cells were either cultured in the control conditions for 24 hrs or with 30ng/ml Wnt3a, rinsed twice with PBS and lysed for 5 min on ice in 400 µl of Cell Lysis Buffer (Cell Signaling) and a cocktail of protease inhibitors (Roche). For detection of Apc and β-catenin proteins by Western blot, whole cell lysates were loaded on a 4–20% linear gradient Tris-HCl Gel (BIO-RAD), and transferred onto PVDF membranes (Millipore) by 1 hr electroblotting at 300 mA constant current at RT in blotting buffer (BIO-RAD). Following transfer, the membranes were blocked with 5% nonfat dry milk in TPBS (0.05% Tween 20 in PBS) for 1 hr. Incubation with primary antibodies was performed overnight at 4°C using rabbit polyclonal anti-Apc (1:100; Abcam) or mouse monoclonal anti-β-catenin (1:2000; Epitomics) antibodies. Blots were washed 3 times with PBS and incubated with horseradish peroxidase-conjugated secondary antibodies for 1 hr at room temperature. The peroxidase was visualized and quantified by enhanced chemiluminescence using the Molecular Imager Gel Doc XR+ System (BIO-RAD).

Real-time quantitative PCR

Real-time quantitative PCR was performed using QuantiTect real-time PCR primers (Qiagen) for the detection of the mouse *Apc*, *Ctnnb1*, *Axin2*, *Smad1*, *Smad3*, *Smad4*, *and Bmp7* genes and analyzed as described previously (16).

Proliferation assay

For proliferation assays, the CellTiter 96® AQueous Non-Radioactive Cell Proliferation Assay (Promega) was used. Cells were seeded at a density of 2,500 cells/cm^2. After 24, 48, 72 and 96 hours, 20 µl of MTS [3-(4,5-dimethylthiazol-2-yl)-5-(3-carboxymethoxyphenyl)-2-(4-sulfophenyl)-2H-tetrazolium)] was added to the medium and the mitochondrial activity was measured at 490 nm after 2 hr incubation at 37°C.

Apoptosis assay

For detection of apoptotic cells, Annexin V staining was performed using Annexin V-FITC (1:250; Bender Med Systems), which specifically binds phosphatidyl serine (PS) residues on the cell membrane, and propidium iodide (PI; Bender Med Systems) at 1µg/ml which binds to DNA once the cell membrane has become permeable. Cells were analyzed by flow cytometry (FACS-Calibur, Becton Dickinson) using the CellQuest program (FACS-Calibur, Becton Dickinson).

Luciferase transient transfection assays

The KSFrt-Apc_{si} and KSFrt-mtApc_{si} stable cells were seeded at a density of 19,000 cells/cm^2 and 9,500 cells/cm^2, respectively, in 24-well plates, and transiently trans-

fected with 2 μg of the reporter construct (pGL3-$(BRE)_2$-Luc, BAT-Luc or pSAR-MT-APC) using Fugene HD transfection reagent (Roche), according to the manufacturer's protocol. To correct for transfection efficiency, 25 ng of Renilla luciferase (pGL4-CAAGS; Promega) was co-transfected. Twenty-four hours after transfection, transfected cells were either left non-stimulated or stimulated for an additional 24 hrs. Luciferase assays were performed as described previously (16).

Differentiation assays

To induce osteogenic differentiation, the KSFrt-*Apc*$_{si}$ and KSFrt-mt*Apc*$_{si}$ stable cells were seeded at a density of 24,000 cells/cm^2 and 12,000 cells/cm^2, respectively, and cultured in the presence or absence of BMP-7 at the concentrations indicated. The medium was changed every 3 to 4 days. At confluence (from Day 4 of culture onward), ascorbic acid (50 μg/ml; Merck) and, when nodules appeared (from Day 11 of culture onward), β-glycerol phosphate (5 mM; Sigma) were added to the culture medium. Analysis of the Alkaline Phosphatase activity (at Day 11) and the degree of mineralization (at Day 21) was performed as previously described (17).

To induce chondrogenic differentiation, 300,000 cells were pelleted by centrifugation in a round-bottom-well of a 96-well-plate (Corning) and cultured in 250 μl high-glucose DMEM (Gibco), supplemented with 100 U/ml Pen/Strep, 50 μg/ml ascorbic acid (Merck), 40 μg/ml proline (Sigma), 1 mM Pyruvate, 1:100 ITS + Premix (BD Biosciences). During the first 2 weeks of culture, medium was further enriched with 10 ng/ml TGFβ3 (R&D Systems) and 10^{-7} M Dexamethasone (Sigma), while beginning with week 3, 500 ng/ml BMP-6 and 5mM β-glycerol-phosphate (Merck) was added to the medium. The medium was replaced every 3 to 4 days. After 6 weeks of culture, pellets were fixed, embedded in paraffin and sectioned. Sections were stained with Toluidine Blue or immunostained for collagen II as previously described (13). Glycosaminoglycan quantification corrected for DNA after 2, 4 and 6 weeks of culture was performed as previously described (16).

To induce adipogenic differentiation, the KSFrt-*Apc*$_{si}$ and KSFrt-mt*Apc*$_{si}$ stable cells were seeded at a density of 24,000 cells/cm^2 and 12,000 cells/cm^2, respectively, and cultured in the presence of 25 μM Indomethacin after confluence (from Day 4 of culture onward). After 3 weeks of culture, cells were stained with Oil Red O as described previously (17). Quantification of adipocytes was performed by counting adipocytes, defined by the presence of at least 3 lipid droplets per cell from 9 randomly selected fields (3 fields/well) for each group.

Statistics

All values represent mean ± SEM of two or three independent triplicate experiments. Differences were examined by one way analysis of variance (ANOVA). Results were considered significant at $p < 0.05$.

RESULTS

The KSFrt-Apc$_{si}$ cell line is a valid model for studying the role of Apc in SPC differentiation

To study the role of the *Apc* gene in regulating lineage commitment and differentiation of SPC, we generated a cell line with decreased Apc expression by RNA interference (RNAi) using the 4C3 Frt clone of the KS483 murine host cell line (18).

Overexpression of *Apc*$_{si}$ but not of mt*Apc*$_{si}$ decreased wild-type Apc protein levels with approximately 50%, suggesting an efficient gene knockdown at the protein level (Figure 1B). KSFrt-*Apc*$_{si}$ cells also showed less total β-catenin protein expression in comparison to control mt*Apc*$_{si}$ cells in whole cell extracts (Figure 1C). Nevertheless, total β -catenin levels were reduced in both cytoplasmic and nuclear cell fractions (data not shown). Treatment with Wnt3a did not affect the Apc expression, but upregulated β-catenin in both KSFrt-*Apc*$_{si}$ and KSFrt-mt*Apc*$_{si}$ cells.

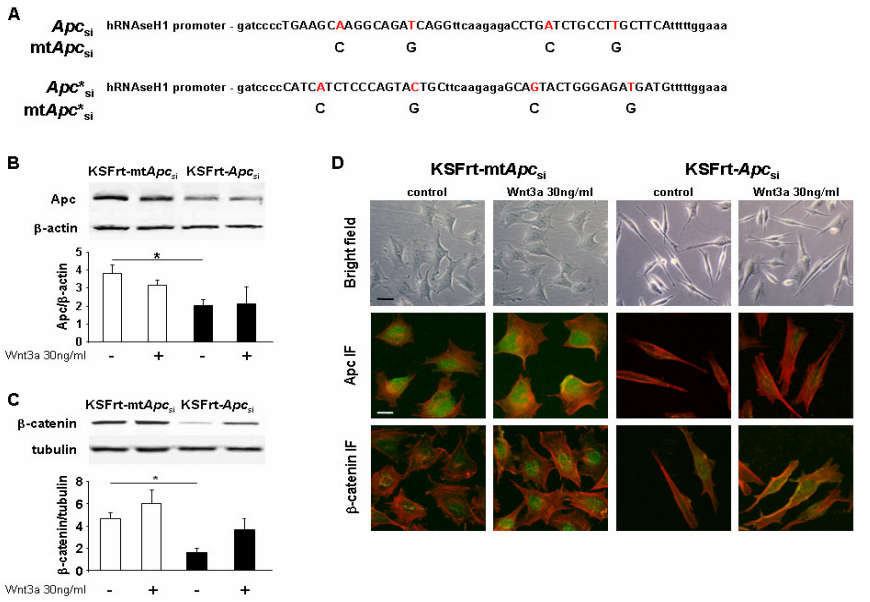

Figure 1. Morphological and structural characterization of the KSFrt-*Apc*$_{si}$ cell line. (A) The Apc target sequence of *Apc*$_{si}$, mt*Apc*$_{si}$, *Apc**$_{si}$, and mt*Apc**$_{si}$ RNAi vectors driven by the hRNAseH1 promoter used to obtain the KSFrt-*Apc*$_{si}$, KSFrt-mt*Apc*$_{si}$, KSFrt-*Apc**$_{si}$, and KSFrt-mt*Apc**$_{si}$ cell line, respectively. (B, C) Quantified western blot analysis, performed on total protein lysates, demonstrated that KSFrt-*Apc*$_{si}$ cells (black bars) express less Apc and β-catenin protein in comparison to control KSFrt-mt*Apc*$_{si}$ cells (white bars). (D) Bright field (upper row), IF for Apc (green; middle row) and for β-catenin (green; lower row) pictures of the control KSFrt-mt*Apc*$_{si}$ and of the KSFrt-*Apc*$_{si}$ cells coupled with Phalloidin staining for the F-actin cytoskeleton (red). Note the spindle shape mesenchymal-like morphology of the KSFrt-*Apc*$_{si}$ cells, expressing less Apc and mostly nuclear β-catenin. Wnt3a (30ng/ml) induced neither morphological nor structural changes in the KSFrt-*Apc*$_{si}$ cells. Bar represents 50 µm (bright field pictures) or 20 µm (IF pictures). *$p < 0.05$.

The morphology of the KSFrt-*Apc*$_{si}$ cells was considerably changed into thin, elongated, spindle shape mesenchymal-like cells in contrast to control cells that maintained the polygonal, cuboidal shape of the parental 4C3 cell line (Figure 1D, upper row). Morphology was not influenced by treatment with Wnt3a in neither of the cell lines. To investigate the cellular level and distribution of Apc and β-catenin in the KSFrt-*Apc*$_{si}$ cells, we next performed immunofluorescence (IF) analysis coupled with Phalloidin staining for visualizing the F-actin cytoskeleton in non-confluent cultures. IF for Apc confirmed the WB results, indicating overall less Apc expression in KSFrt-*Apc*$_{si}$ cells in comparison to control cells (Figure 1D, middle row). Wnt3a affected neither the level of Apc nor its cellular distribution in both cell lines. In control cells, β-catenin was mainly membrane-bound and cytoplasmic, while stimulation with Wnt3a induced β-catenin nuclear translocation (Figure 1D, lower row). In contrast, in the KSFrt-*Apc*$_{si}$ cells, β-catenin was mainly present in the nucleus in both non- and Wnt3a-stimulated conditions. Similar results were obtained on confluent cultures of both cell lines (data not shown).

Functional characterization of the KSFrt-Apc$_{si}$ cell line

Proliferation of both KSFrt-*Apc*$_{si}$ and KSFrt-*Apc**$_{si}$ cells was significantly reduced after 24, 48, 72 and 96 hrs of culture in comparison to control cells, as confirmed by MTS proliferation assay ($p < 0.01$ at all time points; Figure 2A and data not shown). The percentage of apoptotic cells detected by Annexin V staining was significantly increased in the KSFrt-*Apc*$_{si}$ cells as compared to control cells (18.02% and 2.73%, respectively, $p < 0.05$; Figure 2B).

We next used the Wnt responsive BAT-Luc reporter construct to evaluate the effect of *Apc* knockdown on Wnt responsiveness (19). In basal conditions, the reporter activity was significantly increased in the KSFrt-*Apc*$_{si}$ cells in comparison to control cells ($p < 0.01$; Figure 2C), suggestive for increased endogenous canonical Wnt signaling. Remarkably, the response to Wnt3a was blunted in the KSFrt-*Apc*$_{si}$ cell line. This could be due to the lower total β-catenin levels (Figure 1C) and relatively higher percentage of active β-catenin over total β-catenin which already resides in the nucleus of the KSFrt-*Apc*$_{si}$ cells even in basal conditions (Figure 1D). We next examined whether *Apc* knockdown could be rescued by transient transfection of an *APC* expression vector, which induces the expression of wild-type APC in the presence of $ZnCl_2$ (20). As expected, pSAR-MT-APC induced a dose-dependent decrease in BAT-Luc reporter activity in Wnt3a-, but not in non-stimulated control cells. Wild-type APC expression in the KSFrt-*Apc*$_{si}$ cells decreased the high basal Wnt-reporter activity dose-dependently (0μM *vs*. 100μM $ZnCl_2$, $p < 0.05$) and rescued the ability of Wnt3a to activate the BAT-Luc reporter indicative for a partial rescue of the knock down phenotype. Upregulation of the established Wnt/β-catenin target gene *Axin2* at the mRNA level further confirmed the increased canonical Wnt signaling in the KSFrt-*Apc*$_{si}$ cells ($p < 0.01$; Figure 2D) in line with β-catenin immunofluorescence and BAT-LUC reporter assays (21).

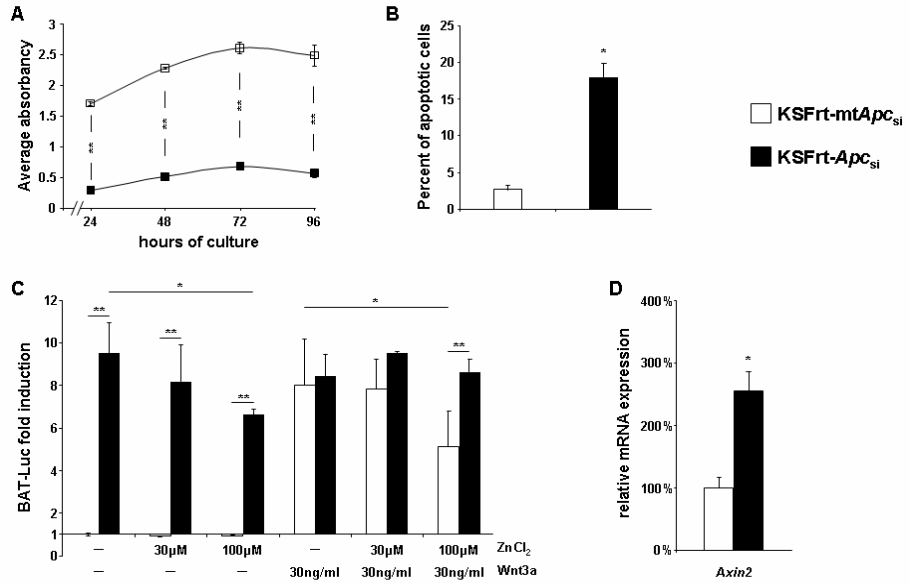

Figure 2. KSFrt-*Apc*$_{si}$ cells display decreased proliferation rate, increased apoptosis and increased Wnt/β-catenin signal transduction. (A) KSFrt-*Apc*$_{si}$ cells (black circles) proliferate significantly less in comparison to control KSFrt-mt*Apc*$_{si}$ cells (white squares), as measured with an MTS proliferation assay. (B) KSFrt-*Apc*$_{si}$ cells (black bar) show significantly increased apoptosis in comparison to control KSFrt-mt*Apc*$_{si}$ cells (white bar), as determined by Annexin V staining. (C) KSFrt-mt*Apc*$_{si}$ (white bars) and KSFrt-*Apc*$_{si}$ cells (black bars) were transiently co-transfected with BAT-Luc and pSAR-MT-APC. In comparison to control KSFrt-mt*Apc*$_{si}$ cells, KSFrt-*Apc*$_{si}$ cells display increased endogenous BAT-Luc activity that is rescued by inducible expression of wild-type APC dose-dependently. No further increase in BAT-Luc activity is observed in KSFrt-*Apc*$_{si}$ cells after stimulation with Wnt3a. Values are expressed as fold induction of firefly luciferase activity of untreated control KSFrt-mt*Apc*$_{si}$ cells. (D) The relative mRNA expression of *Axin2* in the KSFrt-*Apc*$_{si}$ cells (black bar) is higher as compared to KSFrt-mt*Apc*$_{si}$ cells (white bar). *p < 0.05, **p < 0.01.

KSFrt-Apc$_{si}$ cells display an altered differentiation potential to the chondrogenic, adipogenic and osteogenic lineage

We next examined the multipotency of the KSFrt-*Apc*$_{si}$ cells. To determine the potential of KSFrt-*Apc*$_{si}$ cells to differentiate into chondrocytes, we cultured them as pellets for 6 weeks. Throughout the chondrogenic differentiation experiment, all KSFrt-mt*Apc*$_{si}$ pellets remained compact spheres, whereas some of KSFrt-*Apc*$_{si}$ gradually lost their spherical shape and others disintegrated. At the end of the culture period, KSFrt-mt*Apc*$_{si}$ pellets displayed a matrix rich in both Toluidine Blue-positive glycosaminoglycans (GAGs) and Collagen II protein (Figure 3A). In marked contrast, KSFrt-*Apc*$_{si}$ cells did not form a cartilage matrix and did not express Collagen II. GAG quantification corrected for DNA in pellets after 2, 4 and 6 weeks of culture confirmed these observations (Figure 3B). At all time points, we detected significantly lower GAG contents in

the KSFrt-*Apc*$_{si}$ pellets in comparison to controls ($p < 0.05$ at 2 weeks, $p < 0.01$ at 4 and 6 weeks).

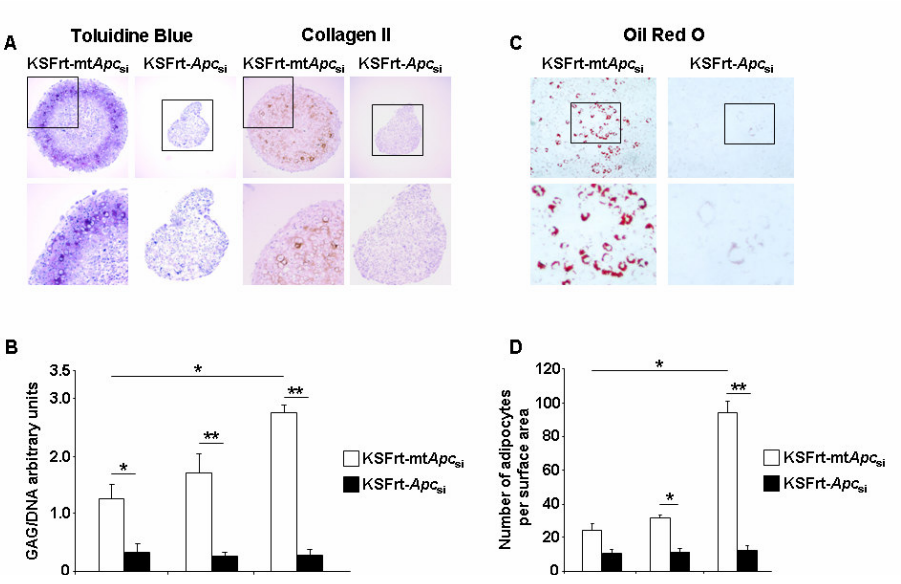

Figure 3. KSFrt-*Apc*$_{si}$ cells display neither chondrogenic nor adipogenic differentiation potential. (A) KSFrt-*Apc*$_{si}$ cells do not differentiate into chondrocytes as demonstrated by the absence of Toluidine Blue staining and Collagen II immunostaining performed after the 6-week-long chondrogenic differentiation protocol. The boxed regions in the pictures of the upper row are magnified in the lower row. (B) Quantification of GAGs corrected for DNA validates the microscopical findings. The GAG content in the KSFrt-mt*Apc*$_{si}$ pellets (white bars) increases time dependently, whereas it remains significantly lower in the KSFrt-*Apc*$_{si}$ pellets (black bars) at all time points. (C) KSFrt-*Apc*$_{si}$ cells do not differentiate into adipocytes as demonstrated by Oil Red O staining performed after the 3-week-long adipogenic differentiation protocol. (D) Adipocyte counting indicates a significantly lower number of adipocytes among the KSFrt-*Apc*$_{si}$ cells per surface area (black bars) when compared to KSFrt-mt*Apc*$_{si}$ cells. *$p < 0.05$, **$p < 0.01$.

The adipogenic differentiation potential of the KSFrt-*Apc*$_{si}$ cells was investigated by performing Oil Red O staining on cells cultured for 1, 2 and 3 weeks in adipogenic medium. After 3 weeks of culture, many of the KSFrt-mt*Apc*$_{si}$ cells differentiated into adipocytes containing lipid droplets that positively stained with Oil Red O (Figure 3C). In contrast, differentiation of KSFrt-*Apc*$_{si}$ cells into adipocytes was severely impaired. Quantification of the number of adipocytes indicated that after 1, 2 and 3 weeks the number of Oil Red O-positive cells was significantly lower in the KSFrt-*Apc*$_{si}$ cells in comparison to controls ($p < 0.05$ at 2 weeks, $p < 0.01$ at 3 weeks; Figure 3D).

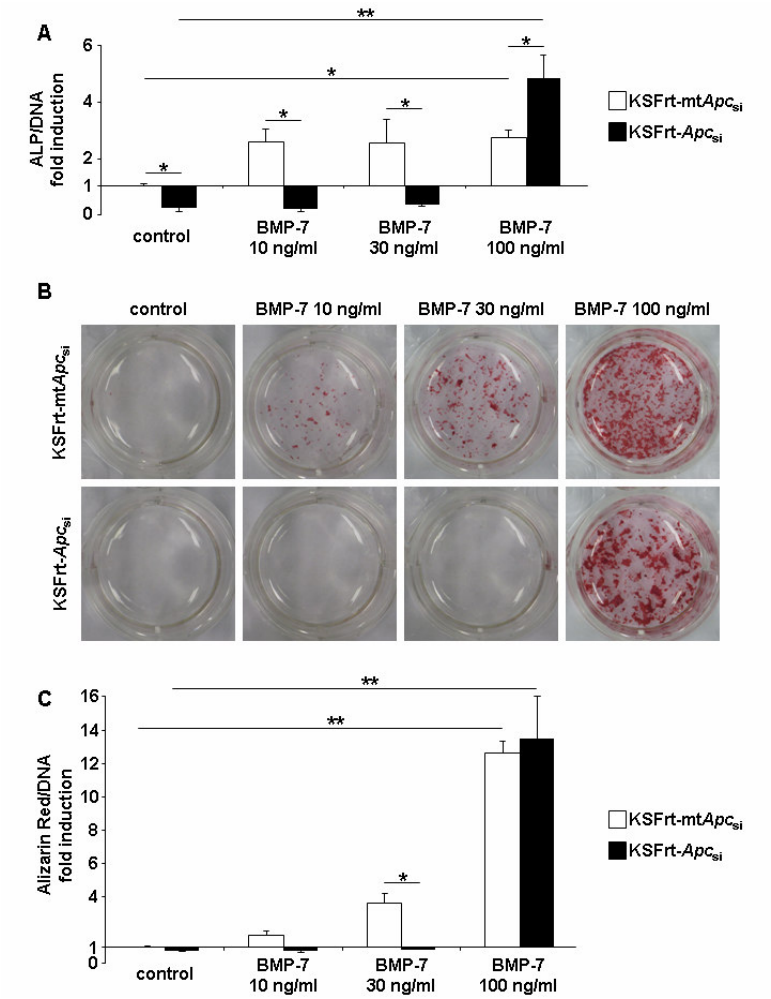

Figure 4. KSFrt-*Apc*$_{si}$ cells display an impaired osteogenic differentiation potential that can be counteracted by high concentrations of BMP-7. (A) Alp activity after 11-day-long osteoblast differentiation protocol. In the absence and at low concentrations of BMP-7, KSFrt-*Apc*$_{si}$ cells (black bars) display significantly less Alp activity in comparison to control KSFrt-mt*Apc*$_{si}$ cells (white bars). When stimulated with 100 ng/ml BMP-7, KSFrt-*Apc*$_{si}$ cells show significantly increased osteogenic differentiation potential in comparison to control KSFrt-mt*Apc*$_{si}$ cells. Values are expressed as fold induction of Alp activity corrected for DNA of untreated control KSFrt-mt*Apc*$_{si}$ cells. (B) Representative images of Alizarin Red S-stained cultures after 21-day-long osteoblast differentiation protocol. BMP-7 stimulates the formation of mineralized nodules dose-dependently in control KSFrt-mt*Apc*$_{si}$ cells, whereas KSFrt-*Apc*$_{si}$ cells show mineralized nodules only in the presence of high BMP-7 concentrations. (C) Quantification of the amount of Alizarin Red corrected for DNA. When treated with 100 ng/ml BMP-7, KSFrt-*Apc*$_{si}$ cells (black bars) show significantly increased mineral deposition in comparison to control condition. Values are expressed as fold induction of Alizarin Red S content corrected for DNA of untreated control KSFrt-mt*Apc*$_{si}$ cells (white bars). *$p < 0.05$, **$p < 0.01$.

To determine the osteogenic potential of KSFrt-*Apc*$_{si}$ cells, we performed short-term osteoblast differentiation experiments. Alkaline Phosphatase (ALP) staining and its consequent quantification indicated that, in comparison to control cells, both KSFrt-*Apc*$_{si}$ and KSFrt-*Apc**$_{si}$ cells display a significantly decreased potential to differentiate into osteoblasts (Figure 4A and data not shown). We next tested whether the inhibition of osteoblastogenesis in the KSFrt-*Apc*$_{si}$ cells could be rescued by the addition of pro-osteogenic growth factors like Basic fibroblast growth factor (bFGF), Transforming growth factor, beta 3 (TGF-β3), Parathyroid hormone-related peptide (PTHrP), Insulin-like growth factor 1 (IGF-1), and 2 members of the BMP family, BMP-6 and BMP-7. Of these, only BMP-7 (and, to a lesser extent, BMP-6) could rescue the *Apc*$_{si}$-mediated inhibition of osteogenic differentiation (Figure 4A and data not shown). Osteoblast maturation of KSFrt-*Apc*$_{si}$ cells was investigated by alizarin Red S staining after long-term cultures to depict mineralization of the osteoblast nodules. Similar to their controls, neither KSFrt-*Apc*$_{si}$ nor KSFrt-*Apc**$_{si}$ cells displayed mineralized nodules in the absence of BMP-7 (Figure 4B and data not shown). In contrast to KSFrt-*Apc*$_{si}$ cells, low concentrations of BMP-7 (10 and 30 ng/ml) were sufficient to induce matrix mineralization in control cells. Interestingly, high concentrations of BMP-7 (100ng/ml) efficiently induced the formation of alizarin Red S-positive nodules in the KSFrt-*Apc*$_{si}$ cells. No statistically significant difference was found when the alizarin Red S staining was quantified between KSFrt-*Apc*$_{si}$ and control cells cultured in the presence of 100ng/ml BMP-7 (Figure 4C). However, the osteoblast nodules formed by the KSFrt-*Apc*$_{si}$ cells were bigger in comparison to those formed by control cells.

Increased BMP signaling in the KSFrt-Apc$_{si}$ cells

We next assessed the level of BMP signaling in the KSFrt-*Apc*$_{si}$ cells by performing transient transfection assays using the BMP-responsive pGL3-$(BRE)_2$-Luc reporter construct (22). KSFrt-*Apc*$_{si}$ cells displayed significantly increased endogenous levels of BMP signaling in comparison to control KSFrt-mt*Apc*$_{si}$ cells ($p < 0.01$; Figure 5A). BMP-7 activated the $(BRE)_2$-Luc reporter dose-dependently in control cells in contrast to KSFrt-*Apc*$_{si}$ cells. In these latter cells, only a high BMP-7 concentration activated the reporter compared to the control condition. The response was blunted in the KSFrt-*Apc*$_{si}$ cells compared to KSFrt-mt*Apc*$_{si}$ cells (0.5-fold *vs.* 4-fold increase, respectively). Noggin, a potent inhibitor of the BMP signaling pathway (7), managed to decrease both the endogenous and the BMP-7-induced activity of the $(BRE)_2$-Luc reporter in the KSFrt-*Apc*$_{si}$ cells, suggestive for autocrine stimulation of the BMP signaling pathway for example by increased expression of BMPs. Upregulation of the BMP signaling pathway in the KSFrt-*Apc*$_{si}$ cells was further confirmed at the mRNA level by quantitative RT-PCR. *Smad1*, *Smad3*, and *Smad4* were significantly increased in the KSFrt-*Apc*$_{si}$ cells ($p < 0.05$; Figure 5B). Interestingly, *Bmp7* showed a 4.4-fold higher expression at the mRNA level in the KSFrt-*Apc*$_{si}$ cells in comparison to KSFrt-mt*Apc*$_{si}$ cells ($p < 0.01$).

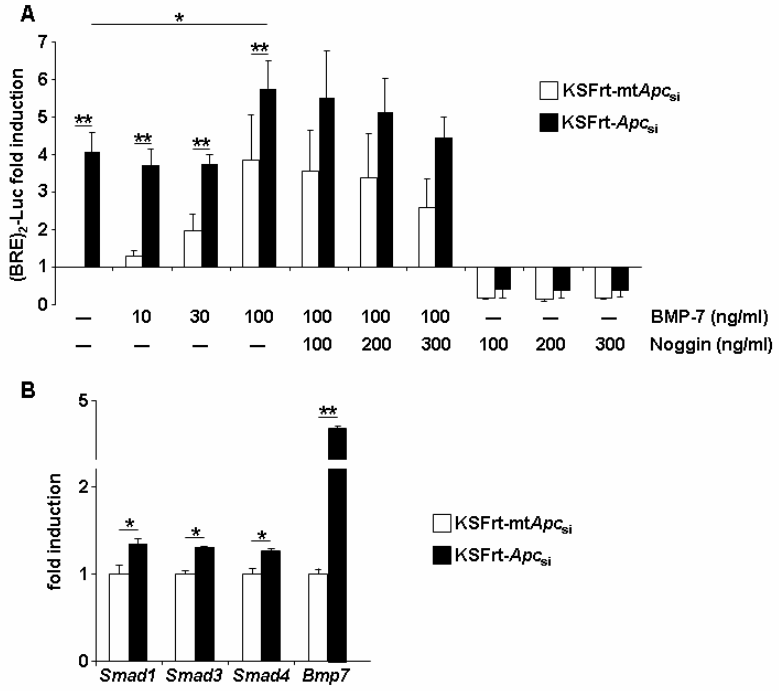

Figure 5. Increased BMP signaling in the KSFrt-*Apc*$_{si}$ cells. (A) KSFrt-mt*Apc*$_{si}$ (white bars) and KSFrt-*Apc*$_{si}$ cells (black bars) were transiently transfected with pGL3-(BRE)$_2$-Luc. KSFrt-*Apc*$_{si}$ cells display increased endogenous (BRE)$_2$-Luc activity that is enhanced by treatment with only high concentrations of BMP-7. Noggin inhibits both the endogenous and the BMP-7-induced (BRE)$_2$-Luc activity in the KSFrt-*Apc*$_{si}$ cells. Values are expressed as fold induction of firefly luciferase activity of untreated control KSFrt-mt*Apc*$_{si}$ cells. (B) Significantly increased relative mRNA expression of *Smad1*, *Smad3*, *Smad4*, and *Bmp7* in KSFrt-*Apc*$_{si}$ cells (black bars) in comparison to KSFrt-mt*Apc*$_{si}$ cells (white bars). *$p < 0.05$, **$p < 0.01$.

DISCUSSION

APC is a multifunctional protein involved in cell adhesion, mitosis, apoptosis, cytoskeletal organization, microtubule assembly, cell fate determination and chromosomal stability, yet it remains mostly investigated as the key intracellular gate-keeper of the canonical Wnt/β-catenin signaling pathway (23-25). In our present study, we demonstrate that Apc is required for proliferation, suppression of apoptosis and differentiation of murine mesenchymal stem cell-like KS483 cells into the osteogenic, chondrogenic and adipogenic lineage. We obtained similar results by using 2 different shRNA sequences targeting *Apc*, while stable transfection of the respective control mutant shRNA plasmids (containing 2 nucleotide mismatches) did not alter the proliferation, survival and differentiation capacity of KS483 cells. This clearly indicates that

our results were the consequence of a bona-fide and specific siRNA effect lowering wild-type Apc expression. This was further confirmed by the partial rescue of BAT-Luc reporter activity by transient transfection of a human *APC* expression vector. Interestingly, KSFrt-*Apc*$_{si}$ cells displayed not only high levels of the canonical Wnt/β-catenin pathway, but also augmented BMP signaling, further sustaining the multifaceted interaction between these two signaling pathways during the differentiation of SPC.

RNAi is a complex biological mechanism during which shRNAs act either by cleavage ("slicing") or by translational repression of their target mRNA (26). KSFrt-*Apc*$_{si}$ cells showed decreased Apc expression at the protein level, thereby documenting an efficient *Apc* knockdown by RNAi (27;28). B-catenin protein expression was also lower in comparison to control cells, suggesting, as has been reported in other cell lines, that low levels of Apc are sufficient to downregulate β-catenin (29). Lower β-catenin expression due to *Apc* knockdown contrasts observations in tumors, in which *Apc* inactivation due to deletion or mutation is linked to increased β-catenin expression (24). In contrast to these models, KSFrt-*Apc*$_{si}$ still expresses wild type Apc albeit at lower levels. Furthermore, cells carrying hypomorphic *Apc* mutations show up-regulation of β-catenin levels only when the Apc activity is reduced below 2% of the normal levels (14). Interestingly, the increased activity of the BAT-Luc Wnt responsive construct in the KSFrt-*Apc*$_{si}$ cells implies a shift of the inactive/active β-catenin balance in favor of the active fraction. The partial rescue of the *Apc*$_{si}$-induced Wnt activation after transfection with an APC expression vector demonstrates that the upregulation of the Wnt signal in the KSFrt-*Apc*$_{si}$ cells is due to *Apc* knockdown. We recently described that the 4C3 Frt clone of the parental KS483 murine mesenchymal progenitor line can differentiate into osteoblasts, chondrocytes and adipocytes, when cultured in the appropriate conditions and represents a valuable biological tool for the evaluation of gene function both *in vivo* and *in vitro* (15;18;30). Thus, the KSFrt-*Apc*$_{si}$ cell line is a reliable model to study the role of Apc in regulating differentiation of SPC (18). It is well established that APC modulates cell shape by organizing the cytoskeleton in particular through stabilization of microtubules (31). The KSFrt-*Apc*$_{si}$ cell line developed elongated cellular protrusions, thereby displaying a clearly distinct morphology from the control cells. In agreement with this, upregulation of the canonical Wnt signal has been shown to promote a spindle-like cell morphology (13;32;33).

It is generally accepted that Apc inhibits cell proliferation via β-catenin-dependent and -independent actions, and that inactivation of *APC* represents the early, initiating event in several malignant diseases (34-36). However, evidence is also available suggesting that APC is essential for cell proliferation (29). Likewise, no consensus regarding the effect of APC on apoptosis has been reached since both stimulation and inhibition of apoptosis by APC have been described (20;37-39). The role of APC in apoptosis, such as observed in the KSFrt-*Apc*$_{si}$ can be either β-catenin dependent or independent (23;38). Based on these results, we currently favor the hypothesis that Apc plays opposing roles during development and malignant transformation, by modulating cell shape, proliferation, and survival in a context dependent manner, with distinct consequences in different cell types and at different developmental stages.

The canonical Wnt/β-catenin signaling pathway governs the lineage commitment of bi-potential SPC into osteoblasts or chondrocytes (40). Roughly, it is proposed that

upregulation of this pathway induces the differentiation of SPC into precursors of the osteogenic lineage, whereas its downregulation is needed for chondrogenic differentiation (5). Data available from *in vivo* and *ex vivo* studies indicate that the osteogenic differentiation potential is altered when Apc is lacking or mutated, even if the resulting levels of β-catenin are high (13;14). Although being exposed to higher levels of transcriptionally active Wnt and BMP signaling, KSFrt-*Apc*$_{si}$ cells display a diminished osteogenic differentiation potential. Similar findings were made in conditional *Apc* knockout mice, in which inactivation of *Apc* in SPCs completely blocked osteoblast and chondrocyte differentiation particular in early stages of skeletogenesis (13). The latter study has also shown that the inhibitory phase in some skeletal elements is followed by accelerated osteoblast formation in later developmental stages (13). Complete inhibition of osteogenesis by knock down of *Apc* appears in contrast with increased BMD and high incidence of osteoma in FAP patients carrying a heterozygous inactivating mutation of *APC* (41). In addition, conditional *Apc* knock out using *Cre* expression under the influence of the *Osteocalcin* promoter, a late marker of osteoblast differentiation, results in increased bone formation and lack of osteoclast formation (42). Therefore we hypothesized that the inhibitory effect on osteoblast differentiation in the KSFrt-*Apc*$_{si}$ cells is cell type dependent and may be reversed by environmental factors like exposure to exogenous growth factors.

Interestingly, when the KSFrt-*Apc*$_{si}$ cells were exposed to additional high concentrations of BMP-7 and to a lesser extent BMP-6, both potent stimulators of osteogenesis (43), they displayed an increased potential to form osteoblasts in comparison to control cells. Such rescue effect was not observed when using other pro-osteogenic growth factors like bFGF, TGF-β3, PTHrP, IGF-1. One of the potential interpretations is that BMP signaling further activates canonical Wnt signaling, thus it synergistically induces the osteoblast differentiation in KSFrt-*Apc*$_{si}$ cells. Our results indicate that Apc is essential for the osteogenic differentiation of the KS483 cell line and that the noxious effect of *Apc* knockdown on osteogenesis can be overruled by high BMP signaling induced by BMP-7. Consistently, *in vitro* observations made in C3H10T1/2 cells demonstrate that canonical Wnt signaling itself is not sufficient, but in synergy with BMP signaling it can promote osteoblast differentiation (44).

Both the canonical Wnt and the BMP signaling pathway have been shown to promote osteoblast differentiation, maturation and mineralization (45). However, the complexity of the interactions between these regulatory pathways and the abundance of *in vitro* reports investigating this interrelation in different osteogenic experimental set-ups, complicate its understanding (9;10;44;46-48). The most probable explanation for the wide variety of effects arising upon this interaction is that they represent different aspects of Wnt and BMP functions that are only visible in certain cell types, at specific developmental stages and under particular experimental conditions. Our results add insight to the complexity of interactions between Wnt/β-catenin and BMP signaling during the differentiation of SPC. In vitro, BMPs induce Wnt expression (8;49), whereas Wnt signaling induces BMP expression (46;50), suggesting that both Wnt and BMP signaling may jointly regulate each other in osteoblasts. In the KS483 cells, *Apc* knockdown upregulated not only transduction of the Wnt signal, but also the BMP signaling pathway, most likely via up-regulation of *Bmp7* expression. APC can

shuttle into and out of the nucleus (51;52), and thus a possible Apc-mediated interaction between Wnt and BMP may occur in any of these two subcellular locations. While in the nucleus the Smad/β-catenin/Lef protein complex regulates many shared target genes (53-55), in the cytoplasm, BMP can either impede or stimulate the canonical Wnt signal via Axin (10;56). Since Apc comprises both Axin and β-catenin binding domains, we speculate that Apc might link the Wnt/β-catenin to BMP signaling pathways during osteoblast differentiation of KS483 cells.

Our present results indicate that Apc is essential for osteogenic, chondrogenic and adipogenic differentiation of the murine mesenchymal-like KS483 cell line which has SPC-like characteristics. Our approach has provided a valuable model in which we demonstrate that levels of functional Apc must be tightly controlled for proper modulation of the transcriptionally active β-catenin and BMP-signaling dosage required for multilineage SPC-differentiation *in vitro*.

ACKNOWLEDGEMENTS

We are grateful to Prof. Dr. Peter ten Dijke (Department of Molecular Cell Biology, LUMC, Leiden, The Netherlands) for the pGL3-$(BRE)_2$-Luc reporter construct; Dr. Stefano Piccolo (Department of Medical Biotechnologies, University of Padua, Italy) for the BAT-Luc reporter construct; and Prof. Dr. Bert Vogelstein (The Ludwig Center for Cancer Genetics and Therapeutics, Howard Hughes Medical Institute and Sidney Kimmel Cancer Center at the Johns Hopkins Medical Institutions, Baltimore, Maryland, USA) for the pSAR-MT-APC construct. We thank Prof. Dr. Slobodan Vukicevic, Department of Anatomy, School of Medicine, Zagreb, Croatia, for kindly providing BMP-6 and BMP-7 for our study.

This work was financially supported by an unrestricted educational grant from IPSEN FARMACEUTICA BV to RLM.

REFERENCES

1. Karsenty G. The complexities of skeletal biology. Nature 2003; 423(6937):316-8.
2. Karsenty G, Kronenberg HM, Settembre C. Genetic control of bone formation. Annu Rev Cell Dev Biol 2009; 25:629-48.
3. Liu F, Kohlmeier S, Wang CY. Wnt signaling and skeletal development. Cell Signal 2008; 20(6):999-1009.
4. Clevers H. Wnt/beta-catenin signaling in development and disease. Cell 2006; 127(3):469-80.
5. Hartmann C. A Wnt canon orchestrating osteoblastogenesis. Trends Cell Biol 2006; 16(3):151-8.
6. Bessa PC, Casal M, Reis RL. Bone morphogenetic proteins in tissue engineering: the road from the laboratory to the clinic, part I (basic concepts). J Tissue Eng Regen Med 2008; 2(1):1-13.
7. ten Dijke P. Bone morphogenetic protein signal transduction in bone. Curr Med Res Opin 2006; 22 Suppl 1:S7-11.
8. Chen Y, Whetstone HC, Youn A, Nadesan P, Chow EC, Lin AC et al. Beta-catenin signaling pathway is crucial for bone morphogenetic protein 2 to induce new bone formation. J Biol Chem 2007; 282(1):526-33.
9. Fischer L, Boland G, Tuan RS. Wnt signaling during BMP-2 stimulation of mesenchymal chondrogenesis. J Cell Biochem 2002; 84(4):816-31.
10. Liu Z, Tang Y, Qiu T, Cao X, Clemens TL. A dishevelled-1/Smad1 interaction couples WNT and bone morphogenetic protein signaling pathways in uncommitted bone marrow stromal cells. J Biol Chem 2006; 281(25):17156-63.
11. Chen M, Zhu M, Awad H, Li TF, Sheu TJ, Boyce BF et al. Inhibition of beta-catenin signaling causes defects in postnatal cartilage development. J Cell Sci 2008; 121(Pt 9):1455-65.
12. Yan Y, Tang D, Chen M, Huang J, Xie R, Jonason JH et al. Axin2 controls bone remodeling through the beta-catenin-BMP signaling pathway in adult mice. J Cell Sci 2009; 122(Pt 19):3566-78.
13. Miclea RL, Karperien M, Bosch CA, van der Horst G, van der Valk MA, Kobayashi T et al. Adenomatous polyposis coli-mediated control of beta-catenin is essential for both chondrogenic and osteogenic differentiation of skeletal precursors. BMC Dev Biol 2009; 9:26.
14. Kielman MF, Rindapaa M, Gaspar C, van Poppel N, Breukel C, van Leeuwen S et al. Apc modulates embryonic stem-cell differentiation by controlling the dosage of beta-catenin signaling. Nat Genet 2002; 32(4):594-605.
15. van der Horst G, van der Werf SM, Farih-Sips H, van Bezooijen RL, Lowik CW, Karperien M. Downregulation of Wnt signaling by increased expression of Dickkopf-1 and -2 is a prerequisite for late-stage osteoblast differentiation of KS483 cells. J Bone Miner Res 2005; 20(10):1867-77.

16. Miclea RL, Robanus-Maandag EC, Goeman JJ, Finos L, Bloys H, Löwik CW et al. Inhibition of GSK3-beta induces loss of the chondrocytic phenotype and cartilage matrix degradation through activation of canonical Wnt signaling. Osteoarthritis Cartilage 2011.

17. van der Horst G, Farih-Sips H, Lowik CW, Karperien M. Hedgehog stimulates only osteoblastic differentiation of undifferentiated KS483 cells. Bone 2003; 33(6):899-910.

18. van der Horst G, de Rooij KE, Hoogendam J, Sips HCM, Feitsma AL, Que I et al. Functional genomics, drug screening and biomaterial evaluation using mesenchymal progenitor cells. 2010.

19. Maretto S, Cordenonsi M, Dupont S, Braghetta P, Broccoli V, Hassan AB et al. Mapping Wnt/beta-catenin signaling during mouse development and in colorectal tumors. Proc Natl Acad Sci U S A 2003; 100(6):3299-304.

20. Morin PJ, Vogelstein B, Kinzler KW. Apoptosis and APC in colorectal tumorigenesis. Proc Natl Acad Sci U S A 1996; 93(15):7950-4.

21. Jho EH, Zhang T, Domon C, Joo CK, Freund JN, Costantini F. Wnt/beta-catenin/Tcf signaling induces the transcription of Axin2, a negative regulator of the signaling pathway. Mol Cell Biol 2002; 22(4):1172-83.

22. Korchynskyi O, ten Dijke P. Identification and functional characterization of distinct critically important bone morphogenetic protein-specific response elements in the Id1 promoter. J Biol Chem 2002; 277(7):4883-91.

23. Hanson CA, Miller JR. Non-traditional roles for the Adenomatous Polyposis Coli (APC) tumor suppressor protein. Gene 2005; 361:1-12.

24. Fodde R. The multiple functions of tumour suppressors: it's all in APC. Nat Cell Biol 2003; 5(3):190-2.

25. van Es JH, Giles RH, Clevers HC. The many faces of the tumor suppressor gene APC. Exp Cell Res 2001; 264(1):126-34.

26. Petersen CP, Bordeleau ME, Pelletier J, Sharp PA. Short RNAs repress translation after initiation in mammalian cells. Mol Cell 2006; 21(4):533-42.

27. Doench JG, Petersen CP, Sharp PA. siRNAs can function as miRNAs. Genes Dev 2003; 17(4):438-42.

28. Rao MK, Pham J, Imam JS, MacLean JA, Murali D, Furuta Y et al. Tissue-specific RNAi reveals that WT1 expression in nurse cells controls germ cell survival and spermatogenesis. Genes Dev 2006; 20(2):147-52.

29. Schneikert J, Behrens J. Truncated APC is required for cell proliferation and DNA replication. Int J Cancer 2006; 119(1):74-9.

30. van der Horst G, Farih-Sips H, Lowik CW, Karperien M. Multiple mechanisms are involved in inhibition of osteoblast differentiation by PTHrP and PTH in KS483 Cells. J Bone Miner Res 2005; 20(12):2233-44.

31. Nathke IS. The adenomatous polyposis coli protein: the Achilles heel of the gut epithelium. Annu Rev Cell Dev Biol 2004; 20:337-66.

32. Weeraratna AT, Jiang Y, Hostetter G, Rosenblatt K, Duray P, Bittner M et al. Wnt5a signaling directly affects cell motility and invasion of metastatic melanoma. Cancer Cell 2002; 1(3):279-88.

33. Haertel-Wiesmann M, Liang Y, Fantl WJ, Williams LT. Regulation of cyclooxygenase-2 and periostin by Wnt-3 in mouse mammary epithelial cells. J Biol Chem 2000; 275(41):32046-51.

34. Park KS, Jeon SH, Kim SE, Bahk YY, Holmen SL, Williams BO et al. APC inhibits ERK pathway activation and cellular proliferation induced by RAS. J Cell Sci 2006; 119(Pt 5):819-27.

35. Faux MC, Ross JL, Meeker C, Johns T, Ji H, Simpson RJ et al. Restoration of full-length adenomatous polyposis coli (APC) protein in a colon cancer cell line enhances cell adhesion. J Cell Sci 2004; 117(Pt 3):427-39.

36. Carson DJ, Santoro IM, Groden J. Isoforms of the APC tumor suppressor and their ability to inhibit cell growth and tumorigenicity. Oncogene 2004; 23(42):7144-8.

37. Ahmed Y, Hayashi S, Levine A, Wieschaus E. Regulation of armadillo by a Drosophila APC inhibits neuronal apoptosis during retinal development. Cell 1998; 93(7):1171-82.

38. Benchabane H, Ahmed Y. The adenomatous polyposis coli tumor suppressor and Wnt signaling in the regulation of apoptosis. Adv Exp Med Biol 2009; 656:75-84.

39. Gaspar C, Fodde R. APC dosage effects in tumorigenesis and stem cell differentiation. Int J Dev Biol 2004; 48(5-6):377-86.

40. Hartmann C. Transcriptional networks controlling skeletal development. Curr Opin Genet Dev 2009; 19(5):437-43.

41. Miclea RL, Karperien M, Langers AM, Robanus-Maandag EC, van Lierop A, van der Hiel B et al. APC mutations are associated with increased bone mineral density in patients with familial adenomatous polyposis. J Bone Miner Res 2010; 25(12):2348-56.

42. Holmen SL, Zylstra CR, Mukherjee A, Sigler RE, Faugere MC, Bouxsein ML et al. Essential role of beta-catenin in postnatal bone acquisition. J Biol Chem 2005; 280(22):21162-8.

43. Lavery K, Hawley S, Swain P, Rooney R, Falb D, Aoui-Ismaili MH. New insights into BMP-7 mediated osteoblastic differentiation of primary human mesenchymal stem cells. Bone 2009; 45(1):27-41.

44. Mbalaviele G, Sheikh S, Stains JP, Salazar VS, Cheng SL, Chen D et al. Beta-catenin and BMP-2 synergize to promote osteoblast differentiation and new bone formation. J Cell Biochem 2005; 94(2):403-18.

45. Lian JB, Stein GS, Javed A, van Wijnen AJ, Stein JL, Montecino M et al. Networks and hubs for the transcriptional control of osteoblastogenesis. Rev Endocr Metab Disord 2006; 7(1-2):1-16.

46. Bain G, Muller T, Wang X, Papkoff J. Activated beta-catenin induces osteoblast differentiation of C3H10T1/2 cells and participates in BMP2 mediated signal transduction. Biochem Biophys Res Commun 2003; 301(1):84-91.

47. Kamiya N, Kobayashi T, Mochida Y, Yu PB, Yamauchi M, Kronenberg HM et al. Wnt Inhibitors Dkk1 and Sost are Downstream Targets of BMP Signaling Through the Type IA Receptor (BMPRIA) in Osteoblasts. J Bone Miner Res 2009.

48. Guo X, Wang XF. Signaling cross-talk between TGF-beta/BMP and other pathways. Cell Res 2009; 19(1):71-88.

49. Rawadi G, Vayssiere B, Dunn F, Baron R, Roman-Roman S. BMP-2 controls alkaline phosphatase expression and osteoblast mineralization by a Wnt autocrine loop. J Bone Miner Res 2003; 18(10):1842-53.

50. Winkler DG, Sutherland MS, Ojala E, Turcott E, Geoghegan JC, Shpektor D et al. Sclerostin inhibition of Wnt-3a-induced C3H10T1/2 cell differentiation is indirect and mediated by bone morphogenetic proteins. J Biol Chem 2005; 280(4):2498-502.

51. Henderson BR. Nuclear-cytoplasmic shuttling of APC regulates beta-catenin subcellular localization and turnover. Nat Cell Biol 2000; 2(9):653-60.

52. Neufeld KL, White RL. Nuclear and cytoplasmic localizations of the adenomatous polyposis coli protein. Proc Natl Acad Sci U S A 1997; 94(7):3034-9.

53. Labbe E, Letamendia A, Attisano L. Association of Smads with lymphoid enhancer binding factor 1/T cell-specific factor mediates cooperative signaling by the transforming growth factor-beta and wnt pathways. Proc Natl Acad Sci U S A 2000; 97(15):8358-63.

54. Theil T, Aydin S, Koch S, Grotewold L, Ruther U. Wnt and Bmp signalling cooperatively regulate graded Emx2 expression in the dorsal telencephalon. Development 2002; 129(13):3045-54.

55. Hussein SM, Duff EK, Sirard C. Smad4 and beta-catenin co-activators functionally interact with lymphoid-enhancing factor to regulate graded expression of Msx2. J Biol Chem 2003; 278(49):48805-14.

56. Tang Y, Liu Z, Zhao L, Clemens TL, Cao X. Smad7 stabilizes beta-catenin binding to E-cadherin complex and promotes cell-cell adhesion. J Biol Chem 2008; 283(35):23956-63.